Laser and Particle Beams (2012), *30*, 421–425.
© Cambridge University Press, 2012 0263-0346/12 $20.00
doi:10.1017/S0263034612000304

Electron acceleration in vacuum with two overlapping linearly polarized laser pulses

XIAOSHAN WANG, HONGCHUAN DU, AND BITAO HU
School of Nuclear Science & Technology, Lanzhou University, Lanzhou, China
(RECEIVED 6 January 2012; ACCEPTED 12 April 2012)

Abstract

A novel electron acceleration approach with two overlapping linearly polarized laser pulses in vacuum is proposed. By our simulation, the energy and space spreads can reduce greatly comparing with the acceleration with only one laser pulse having doubled peak laser intensity for realistic laser parameters and the average energy gain from our scheme can be doubled for certain pulse lengths, at the same time. Using numerical simulation, analytical criteria for optimal regimes of our acceleration scheme is found.

Keywords: Electron acceleration; Intense laser pulse; Numerical simulation

INTRODUCTION

Due to the development of chirped-pulse amplification technique, peta-watt short pulse lasers with intensity of 10^{22} W/cm^2 are available in laboratories (Strickl & Mourou, 1985; Perry *et al.,* 1999; Kienberger *et al.,* 2002; Ledingham *et al.,* 2003). Because of the high intensity of the laser field, there has been continuous interest in electron acceleration in vacuum and numerous theoretical and experimental studies (Barton & Alexander, 1989; Esarey *et al.,* 1995*a*; Malka & Miquei, 1996, Malka *et al.,* 1997; Hafizi *et al.,* 1999; Stupakov & Zolotorev, 2000; Salamin & Keitel, 2002; Salamin *et al.,* 2003; Huang & Wu, 2008; Schmid *et al.,* 2009; Lourenco *et al.,* 2010; Smorenburg *et al.,* 2010; Xie *et al.,* 2010; Li *et al.,* 2011) have been performed in this field. However, shortcomings of many of those schemes are that the electron energy spread and the space spread both in transverse and longitudinal directions are very large, especially using linearly polarized laser pulse. Because well-collimated electron beams are required in practical experiments, this limits the applications of those schemes.

It's well known that E_z and $\boldsymbol{\beta} \times \mathbf{B}$ forces contribute significantly to the forward drift and to the rate at which electrons gain energy from the field. For linearly polarized Gaussian pulse, electrons are scattered at large angles and only a small portion can get very high energy. In this work, we propose a novel electron acceleration approach with two overlapping linearly polarized laser pulses in vacuum. The interfere of the two pulses at overlapping parts will produce an electromagnetic field that is totally different with the field of only one pulse. The dynamics of the electron and the acceleration process in this field will be affected. By numerical investigations, we found that our scheme can reduce the transverse scattering during acceleration, which leads to an extremely small space and energy spreads for the electron beam. Furthermore, for certain pulse lengths, average electron energy gained in such acceleration can be doubled comparing with acceleration using only one laser pulse having doubled peak laser intensity for realistic laser parameters.

MODEL AND METHOD

In our scheme, two overlapping pulses, pulse one and two are used to accelerate electrons initially at rest in vacuum. The two pulses are the same in their pulse lengths, wave lengths, waist sides, amplitudes, and polarizations. The relationship of the two pulses is that they are over lapping for δz and pulse two behinds pulse one, as shown in Figure 1. We use the Gaussian functions for the transverse directions for both pulses with the deviations $\omega(z) = \omega_0\sqrt{1 + \left(z/z_r\right)^2}$ for pulse one, where ω_0 is the waist size, z_r is the Rayleigh length, $z_r = k\omega_0^2/2$ with $k = 2\pi/\lambda$ and for pulse two $w'(z) = w(z')$, where $z' = z + \delta z$. For the longitudinal shapes, cosine square forms are adopted instead of Gaussian ones (Esarey *et al.,* 1995*b*; Hua *et al.,* 2004; Karmakar & Pukhov, 2007; Singh *et al.,* 2008). The cosine square

Address correspondence and reprint requests to: Bitao Hu, 222, S. Tianshui Rd, Lanzhou 730000, Gansu, China. E-mail: hubt@lzu.edu.cn

https://doi.org/10.1017/S0263034612000304 Published online by Cambridge University Press

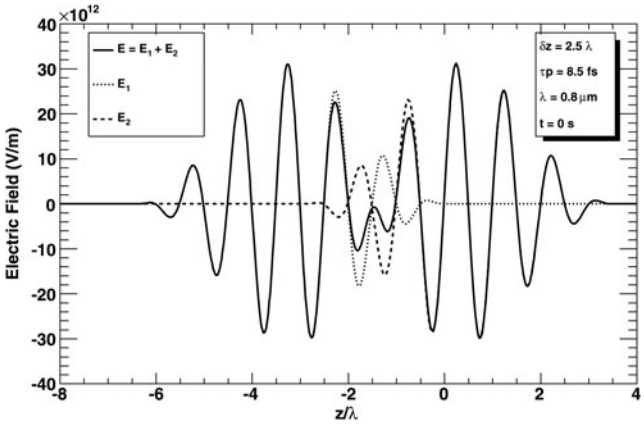


Fig. 1. The electric fields versus z at $t = 0$ and $x = y = 0$. $\mathbf{E_1}$ and $\mathbf{E_2}$ are the fields for pulse one and pulse two, and $\mathbf{E}$ is the total electric field.

forms satisfy the zeroth-order approximation for short laser pulse description for specific spectral distribution function, as Gaussian forms (Esarey *et al.,* 1995*b*; Hua *et al.,* 2004). In our simulation, we have selected linearly polarized Gaussian pulse because it is relatively easy to generate in the laboratory. The electric field of pulse one can be written as

$$\mathbf{E}_1(\mathbf{r}, t) = \mathbf{E}_{G1}(\mathbf{r}, t)\cos^2\frac{(t - z/c - \tau_p)\pi}{2\tau_p}, \tag{1}$$

where τ_p is full width at half maximum (FWHM) pulse length, c is the speed of light in vacuum, $\mathbf{E}_{G1}(\mathbf{r}, t)$ is the electric field of Gaussian beam for pulse one. Substitute z with z' we can obtain the electric field of pulse two

$$\mathbf{E}_2(\mathbf{r}, t) = \mathbf{E}_{G_2}(\mathbf{r}, t)\cos^2\frac{(t - z'/c - \tau_p)\pi}{2\tau_p}, \tag{2}$$

where $\mathbf{E}_{G2}(\mathbf{r},t)$ is electric field of Gaussian beam for pulse two. The total electric field will be presented by

$$\mathbf{E}(\mathbf{r}, t) = \mathbf{E}_1(\mathbf{r}, t) + \mathbf{E}_2(\mathbf{r}, t). \tag{3}$$

Similarly, the magnetic field can be written as

$$\mathbf{B}(\mathbf{r}, t) = \mathbf{B}_1(\mathbf{r}, t) + \mathbf{B}_2(\mathbf{r}, t), \tag{4}$$

where $\mathbf{B}_1 = \mathbf{B}_{G_1}\cos^2\frac{(t - z/c - \tau_p)\pi}{2\tau_p}$ and $\mathbf{B}_2 = \mathbf{B}_{G_2}\cos^2\frac{(t - z'/c - \tau_p)\pi}{2\tau_p}$ are magnetic fields for pulse one and two; $\mathbf{B}_{G_1}$, $\mathbf{B}_{G_2}$ are magnetic fields of Gaussian beams for pulse one and pulse two, respectively.

In our calculation, we use Gaussian pulses polarized along the x axis, propagating along the z axis, of wavelength λ, frequency ω and constant phase ψ_0. The electromagnetic fields are calculated by Eqs. (3) and (4), and Gaussian field components $\mathbf{E_{G1}}$, $\mathbf{E_{G2}}$, and $\mathbf{B_{G1}}$, $\mathbf{B_{G2}}$ are given in Salamin and Keitel (2002) and expressed by

$$E_x = E\left\{S_0 + \epsilon^2\left[\xi^2 S_2 - \frac{\rho^4 S_3}{4}\right] + \epsilon^4\left[\frac{S_2}{8} - \frac{\rho^2 S_3}{4} - \frac{\rho^2(\rho^2 - 16\xi^2)S_4}{16} - \frac{\rho^4(\rho^2 + 2\xi^2)S_5}{8} + \frac{\rho^8 S_6}{32}\right]\right\}, \tag{5}$$

$$E_y = E\xi\nu\left\{\epsilon^2 S_2 + \epsilon^4\left[\rho^2 S_4 - \frac{\rho^4 S_5}{4}\right]\right\}, \tag{6}$$

$$E_z = E\xi\left\{\epsilon C_1 + \epsilon^3\left[-\frac{C_2}{2} + \rho^2 C_3 - \frac{\rho^4 C_4}{4}\right] + \epsilon^5\left[-\frac{3C_3}{8} - \frac{3\rho^2 C_4}{8} + \frac{17\rho^4 C_5}{16} - \frac{3\rho^6 C_6}{8} + \frac{\rho^8 C_7}{32}\right]\right\}, \tag{7}$$

$$B_x = 0, \tag{8}$$

$$B_y = E\left\{S_0 + \epsilon^2\left[\frac{\rho^2 S_2}{2} - \frac{\rho^4 S_3}{4}\right] + \epsilon^4\left[\frac{\rho^2 S_3}{4} - \frac{S_2}{8} + \frac{5\rho^4 S_4}{16} - \frac{\rho^6 S_5}{4} + \frac{\rho^8 S_6}{32}\right]\right\}, \tag{9}$$

$$B_z = E\nu\left\{\epsilon C_1 + \epsilon^3\left[\frac{C_2}{2} + \rho^2 C_3 - \frac{\rho^4 C_4}{4}\right] + \epsilon^5\left[\frac{3C_3}{8} + \frac{3\rho^2 C_4}{8} + \frac{3\rho^4 C_5}{16} - \frac{\rho^6 C_6}{4} + \frac{\rho^8 C_7}{32}\right]\right\}. \tag{10}$$

The paremeters used in Eqs. (5)–(10) are $\xi = x/\omega_0$, $\nu = y/\omega_0$, $\rho = r/\omega_0$, $\epsilon = \omega_0/z_r$, $r = (x^2 + y^2)^{1/2}$, $E = E_0\frac{\omega_0}{\omega}\exp\left(\frac{-r^2}{\omega^2}\right)$, $S_n = \left(\frac{\omega_0}{\omega}\right)^n \sin(\psi + n\psi_G)$, $(n = 0, \quad 1,\ldots,6)$, and $C_n = \left(\frac{\omega_0}{\omega}\right)^n \cos(\psi + n\psi_G)$, $(n = 1, 2, \ldots, 7)$. Also, $E_0 = k\boldsymbol{A}_0$, A_0 is the amplitude of a vector potential; $\psi = \psi_0 + \psi_P + \psi_G - \psi_R$, where ψ_0 is a constant phase, $\psi_P = \eta = \omega t - kz$ is the plane wave phase, $\psi_G = \tan^{-1}(z/z_r)$ is the Guoy phase, $\psi_R = kr^2/(2R)$ is the phase associated with the curvature of the wave fronts, and $R(z) = z + z_r^2/z$ is the radius of curvature of a wave front intersecting the beam axis at the coordinate z. We can use the electromagnetic field expression directly for pulse one, and substituting z with z' for pulse two. We use a dimensionless parameter (Salamin & Keitel, 2002) $q = eE_0/mc\omega$ in our work for convenience. The laser peak intensity I_0 is expressed in q by $I_0 \approx 1.375 \times 10^{18} q^2/\lambda^2$ (W/cm^2), where wavelength λ is in μm.

https://doi.org/10.1017/S0263034612000304 Published online by Cambridge University Press

We discuss the dynamics of electron by numerically solving the Newton-Lorentz equation

$$\frac{\mathrm{d}\mathbf{p}}{\mathrm{d}t} = -e\left[\mathbf{E}+\beta\times\mathbf{B}\right], \tag{11}$$

where, momentum $\mathbf{p} = \gamma mc\beta$, the Lorentz factor $\gamma = (1-\beta^2)^{-0.5}$, $\boldsymbol{\beta}$ is velocity, normalized by the speed of light in vacuum. The energy gain is defined as $(\gamma - \gamma_0)mc^2$, where the energy $\varepsilon = \gamma mc^2$ can be obtained from $d\varepsilon/dt$ equation (Salamin & Keitel, 2002)

$$\frac{\mathrm{d}\varepsilon}{\mathrm{d}t} = -ec\beta\cdot\mathrm{E}. \tag{12}$$

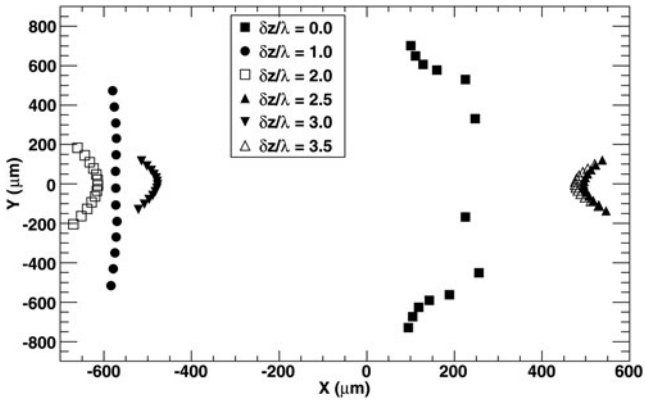


Fig. 3. Space spread in *x*-*y* directions for different δzs. Initial conditions are same for each δz and the interaction time is 8.5 ps.

RESULTS AND DISCUSSION

Firstly, we calculate the average energy gain of $N = 13$ electrons initially at rest and distributed along y axial from -0.5 ω_0 to 0.46 ω_0 with equal intervals of 0.08 ω_0. The parameters of the laser pulses are chosen as wavelengths of 800 nm and FWHM pulse lengths of 8.5 fs, waist sizes 3 μm and peak intensities of $\approx 2.42\times10^{20}$ W/cm^2 for the two pulses. The result is shown versus δz in Figure 2. There are several distinct regions where the average energy gains are comparable to or even larger than that at $\delta z/\lambda = 0$, corresponding to the one pulse acceleration. One can see that the average energy gain value is $\approx 64\%$ larger at the point $\delta z/\lambda = 3.5$ than that at $\delta z/\lambda = 0$.

Figure 3 illustrates space spreads in x, y directions and Figure 4 electron energy gain spread variations with initial positions for $\delta z/\lambda = 0$, 1.0, 2.0, 2.5, 3.0 and 3.5. From Figure 3, it can be seen that space spreads at $\delta z/\lambda = 2.5$, 3.0, 3.5 are significantly small comparing with that at $\delta z/\lambda = 0$, and the spread reduces more than 85% in the y direction especially. From Figure 4, one can see that the energy gain spread reduces from $\approx 270\%$ to $\approx 30\%$ at $\delta z/\lambda = 2.0$, 2.5, 3.0, 3.5, about one-order-of-magnitude decrease.

According to the Lawson-Woodward theorem, the net energy gain of a relativistic electron interacting with electromagnetic filed in vacuum is zero because in a plane wave every accelerating half cycle is followed by an equally decelerating one (Salamin & Keitel, 2002). The Lawson-Woodward theorem conditions can not be satisfied in our investigation because the interaction is limited both in space and time for electron acceleration with the tightly focused laser pulse in vacuum and the non-linear effects are significant and cannot be neglected. In our simulation, the magnetic component of the Lorentz force $\boldsymbol{\beta}\times\mathbf{B}$ becomes comparable to the electric component $\mathbf{E}$ and the electron's velocity $\boldsymbol{\beta}$ initially acquired from $\mathbf{E}$ is modified by $\mathbf{B}$. The electric component E_z and the Lorentz force component $(\boldsymbol{\beta}\times\mathbf{B})_z$ contribute significantly to the forward drift (see Eq. (11)) and the electron energy gain during the acceleration process is determined by Eq. (12).

Figure 5 shows examples of the energy gains versus election longitudinal position z using acceleration with (a) one pulse having doubled peak laser intensity, and (b) two overlapping pulses with a delay of 2.5 λ. The pulse length (FWHM) is 8.5 fs and the maximum accelerating field is

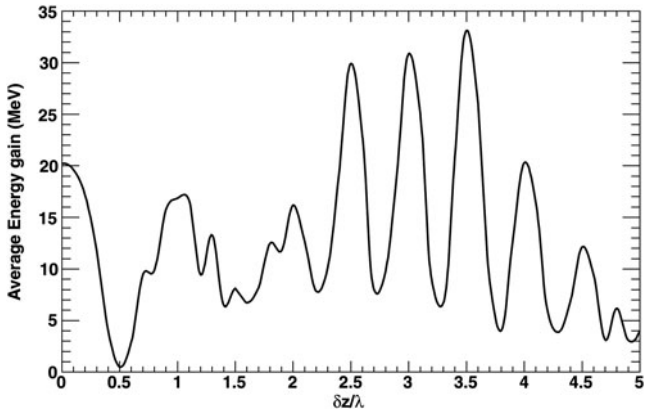


Fig. 2. The average energy gain variation with δz with constant phase $\psi_0 = 0$. The interaction time is 8.5 ps.

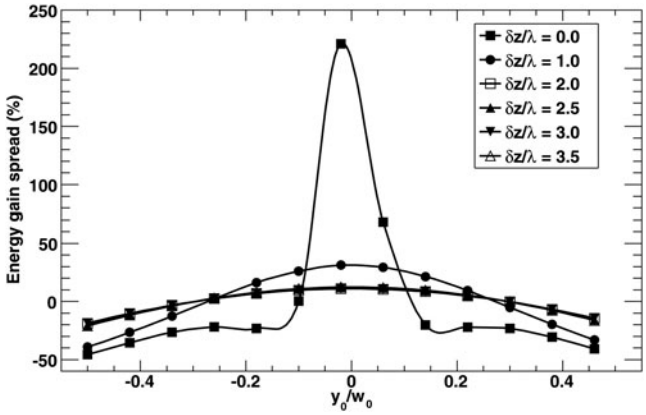


Fig. 4. Energy spread variations with initial positions for different δzs. Initial conditions are the same as Figure 3.

https://doi.org/10.1017/S0263034612000304 Published online by Cambridge University Press

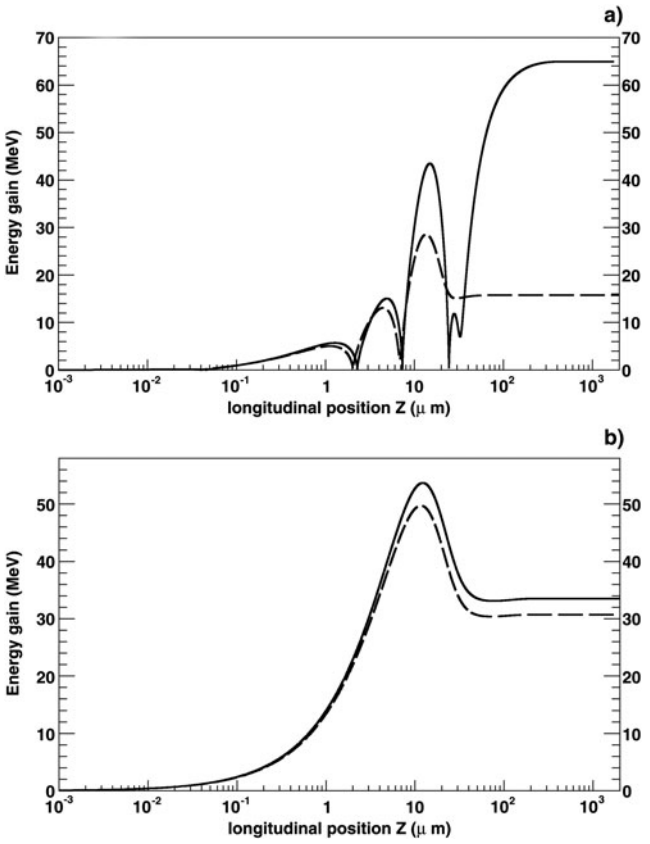


Fig. 5. Examples of the energy gains versus election longitudinal position z: (**a**) acceleration with only one pulse having doubled peak laser intensity, and (**b**) acceleration with the two pulse scheme with a delay of 2.5 λ. The solid and dash line stand for different initial position (0, $-0.02\ \omega_0$, 0) and (0, $-0.26\ \omega_0$, 0), respectively. Other parameters are the same as Figure 2.

about 4.26×10^{13} V/m, corresponding to the peak laser intensity $\approx 2.42 \times 10^{20}$ W/cm^2, for our two pulse acceleration scheme in our calculation. From Figure 5a one can see that for electron acceleration with only one pulse, the accelerating lengths are about 30 and 300 μm in longitudinal direction for different electron initial positions in the example. And the electron undergoes several accelerating-decelerating phases and the main contribution to the final energy gain comes from the last accelerating phase. But the acceleration processes for different initial electron positions are quite distinct except in the early phases because the nonlinear response to the laser field increases with the increasing of laser field amplitude. From Figure 5b , one can see that with our scheme the two acceleration processes for different initial electron positions are very similar to each other and the accelerating lengths are about 50 μm for two different electron initial positions and there is only one accelerating-decelerating phase for individual accelerating process. It can be understood as due to interacting with the overlapping part of the two delayed replicas of laser pulse the electron acquires it's initial velocity dramatically and drifts away from z-axis, which is different from acceleration with one pulse where the field amplitude increases from zero and the

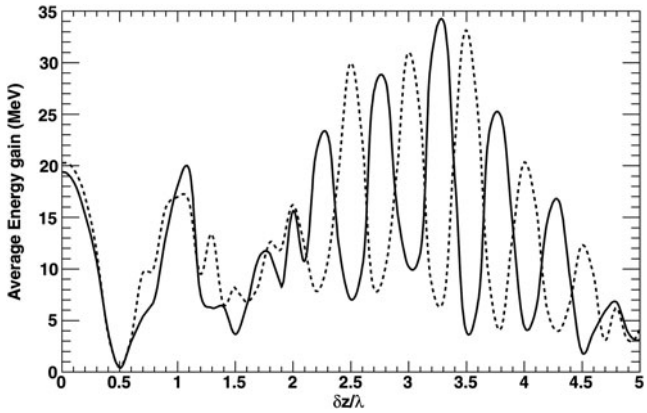


Fig. 6. The average energy gain versus δz. Constant phase ψ_0 is $\pi/2$ (solid line) and π (dashed line). Other parameters are the same as Figure 2.

electron undergoes several accelerating–decelerating phases during the accelerating process. And we attribute the one-order-of-magnitude energy spread decrease to this difference between the two electron acceleration schemes.

Using numerical simulation, we tried to find analytical criteria for the optimal regimes. First, we investigate the effects of constant phase ψ_0 when the other parameters keep unchanged. Figure 6 shows the average energy gains versus δz for $\psi_0 = \pi/2$ (solid line) and π (dashed line). It must be noted that the curves are almost the same for $\psi = 0$ (Fig. 2) and π (Fig. 6, dashed line). One can see that the effects of constant phase ψ_0 are obvious for fixed δz. But the maximum average energy gains for different ψ_0 are affected slightly. The optimal δz changes linearly in one fourth wavelength when ψ_0 changes in a period.

In the following, we study the effects of pulse length τ_p. Figure 7 shows the energy gains versus δz for $\tau_p = 5$ fs and 12 fs pulses. The interaction times are 5 ps and 12 ps, respectively. The interaction times are selected in our calculation to make sure the acceleration processes are finished. The maximum energy gain is gotten at $\delta z/\lambda = 0$ for $\tau_p = 5$ fs, and local maximums at 1.5, 2.0, and 2.5. But the

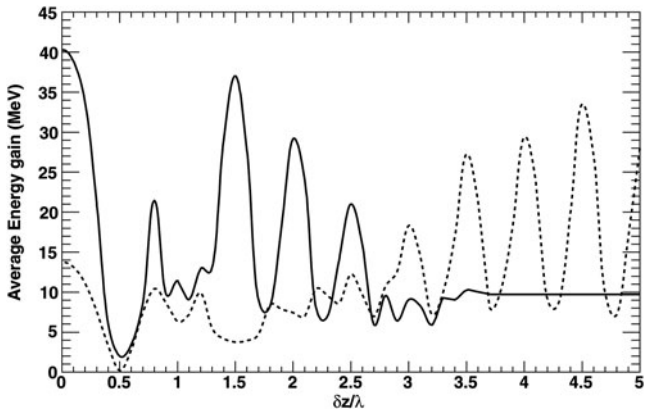


Fig. 7. Same as Fig. 6 for the 5 fs (solid line) and the 12 fs (dashed) pulse. Their interaction times are 5 and 12 ps, respectively. Other parameters are the same as Figure 2.

https://doi.org/10.1017/S0263034612000304 Published online by Cambridge University Press

result is very different for the $\tau_p = 12$ fs pulse (dashed line). The maximum energy gain is gotten at $\delta z/\lambda = 4.5$ and the average energy gained at 0 is less than one-half of the maxima. It means the acceleration efficiency is sufficiently increased with our scheme when the laser pulse duration is longer than several femtoseconds. But for extremely short pulse, our scheme loses effectiveness because the electromagnetic field of the laser pulse changes rapidly.

CONCLUSIONS

In summary, a novel electron acceleration scheme with two linearly polarized overlapping pulses in vacuum has been proposed and investigated numerically. According to our simulation results, smaller the energy and space spreads can be achieved with our acceleration scheme comparing with the one pulse acceleration scheme at the same conditions for realistic laser parameters. The constant phase affects the optimal region in one fourth wavelength and our scheme is more sufficient when the laser pulse lengths longer than several femtoseconds. We can draw the conclusion that our electron acceleration scheme has superiorities comparing with the scheme using only one pulse.

ACKNOWLEDGMENTS

This work was supported by National Natural Science Foundation of China (Grant No.11135002, 11075069, 91026021, 11075068 and 10975065), and the Fundamental Research Funds for the Central Universities (Grant No. lzujbky-2010-k08)

REFERENCES

Barton, J.P. & Alexander, D.R. (1989). Fifth-order corrected electro-magnetic field components for a fundamental Gaussian beam. *J. Appl. Phys*. **66**, 2800–2802.

Esarey, E., Sprangle, P. & Krall, J. (1995*a*). Laser acceleration of electrons in vacuum. *Phys. Rev. E* **52**, 5443–5453.

Esarey, E., Sprangle, P., Pilloff, M. & Krall, J. (1995*b*). Theory and group velocity of ultrashort, tightly focused laser pulses. *J. Opt. Soc. Am. B* **12**, 1695–1703.

Hafizi, B., Ganguly, A.K., Ting, A., Moore, C.I. & Sprangle, P. (1999). Analysis of Gaussian beam and Bessel beam driven laser accelerators. *Phys. Rev. E* **60**, 4779–4792.

Hua, J.F., Ho, Y.K., Lin, Y.Z., Chen, Z., Xie, Y.J., Zhang, S.Y., Yan, Z. & Xu, J.J. (2004). High-order corrected fields of ultrashort, tightly focused laser pulses. *Appl. Phys. Lett*. **85**, 3705–3707.

Huang, S.H. & Wu, F.M. (2008). Electron acceleration by a focused laser pulse in static electric field. *Acta Phys. Sin*. **57**, 7680–7684 (in Chinese).

Karmakar, A. & Pukhov, A. (2007). Collimated attosecond GeV electron bunches from ionization of high-Z material by radially polarized ultra-relativistic laser pulses. *Laser Part. Beams* **25**, 371–377.

Kienberger, R., Hentschel, M., Uiberacker, M., Spielmann, C., Kitzler, M., Scrinzi, A., Wieland, M., Westerwalbesloh, T., Kleineberg, U., Heizmann, U., Drescher, M. & Krausz, F. (2002). Steering attosecond electron wave packets with light. *Science* **297**, 1144–1148.

Ledingham, K.W.D., McKenna, P. & Singhal, R.P. (2003). Applications for nuclear phenomena generated by ultra-intense lasers. *Science* **300**, 1107–1111.

Li, J.X., Fan, X.L., Zang, W.P. & Tian, J.G. (2011). Vacuum electron acceleration driven by two crossed Airy beams. *Opt. Lett*. **36**, 648–650.

Lourenco, S., Kowarsch, W., Scheid, W. & Wang, P.X. (2010). Acceleration of electrons and electromagnetic fields of highly intense laser pulses. *Laser Part. Beams* **28**, 195–201.

Malka, G., Lefebvre, E. & Miquel, J.L. (1997). Experimental observation of electrons accelerated in vacuum to relativistic energies by a high-intensity laser. *Phys. Rev. Lett*. **78**, 3314–3317.

Malka, G. & Miquel, J.L. (1996). Experimental confirmation of ponderomotive-force electrons produced by an ultrarelativistic laser pulse on a solid target. *Phys. Rev. Lett*. **77**, 75–78.

Perry, M.D., Pennington, D., Stuart, B.C., Tietbohl, G., Britten, J.A., Brown, C., Herman, S., Golick, B., Kartz, M., Miller, J., Powell, H.T., Vergino, M. & Yanovsky, V. (1999). Patawatt laser pulses. *Opt. Lett*. **24**, 160–162.

Salamin, Y.I. & Keitel, C.H. (2002). Electron acceleration by a tightly focused laser beam. *Phys. Rev. Lett*. **88**, 095005(4).

Salamin, Y.I., Mocken, G.R. & Keitel, C.H. (2003). Relativistic electron dynamics in intense crossed laser beams: Acceleration and Compton harmonics. *Phys. Rev. E* **67**, 016501(13).

Schmid, K., Veisz, L., Tavella, F., Benavides, S., Tautz, R., Herrmann, D., Buck, A., Hidding, B., Marcinkevicius, A., Schramm, U., Geissler, M., Meyerter-Vehn, J., Habs, D. & Krausz, F. (2009). Few-cycle laser-driven electron acceleration. *Phys. Rev. Lett*. **102**, 124801(4).

Singh, K.P., Sajal, V. & Gupta, D.N. (2008). Quasi-monoenergetic GeV electrons from the interaction of two laser pulses with a gas. *Laser Part. Beams* **26**, 597–604.

Smorenburg, P.W., Kamp, L.P.J., Geloni, G.A. & Luiten, O.J. (2010). Coherently enhanced radiation reaction effects in laser-vacuum acceleration of electron bunches. *Laser Part. Beams* **28**, 553–562.

Strickl, D. & Mourou, G. (1985). Compression of amplified chirped optical pulses. *Opt. Commum*. **56**, 219–211.

Stupakov, G.V. & Zolotorev, M.S. (2000). Ponderomotive laser acceleration and focusing in vacuum for generation of attosecond electron bunches. *Phys. Rev. Lett*. **86**, 5274–5277.

Xie, Y.J., Wang, W., Zheng, L., Zhang, X.P., Kong, Q., Ho, Y.K. & Wang, P.X. (2010). Field structure and electron acceleration in a slit laser beam. *Laser Part. Beams* **28**, 21–26.

https://doi.org/10.1017/S0263034612000304 Published online by Cambridge University Press